



RESEARCH ARTICLE

Near-surface mean wind in Switzerland: Climatology, climate model evaluation and future scenarios

Michael Graf^{1,2} | Simon C. Scherrer³  | Cornelia Schwierz³ | Michael Begert³  |
Olivia Martius^{1,2} | Christoph C. Raible^{2,4} | Stefan Brönnimann^{1,2}

¹Institute of Geography, University of Bern, Bern, Switzerland

²Oeschger Centre for Climate Change Research, University of Bern, Bern, Switzerland

³Climate Division, Federal Office of Meteorology and Climatology MeteoSwiss, Zurich, Switzerland

⁴Climate and Environmental Physics, University of Bern, Bern, Switzerland

Correspondence

Simon C. Scherrer, Operation Center 1, P.O. Box 257, CH-8058 Zurich-Airport, Switzerland.

Email: simon.scherrer@meteoswiss.ch

Funding information

Swiss National Centre for Climate Services (NCCS)

Abstract

Near-surface seasonal and annual mean wind speed in Switzerland is investigated using homogenized observations, Twentieth Century Reanalysis (20CRv2c) data and raw model output of a 75 member EURO-COordinated Downscaling EXperiment regional climate model (RCM) ensemble for present day and future scenarios. The wind speed observations show a significant decrease in the Alps and on the southern Alpine slopes in the period 1981–2010. However, the 20CRv2c data reveal that the recent trends lie well within the decadal variability over longer time periods and no clear signs of a systematic wind stilling can be found for Switzerland. The ensemble of RCMs shows large biases in the annual mean wind speed over the Jura mountains, and some members also show large biases in the Alps compared to station observations. The spatial distribution of the model biases varies strongly between the RCMs, while the resolution and the driving global model have less impact on the pattern of the model bias. The RCMs are mostly able to represent the seasonality of wind speed on the Plateau but miss important details in complex terrain related to local wind systems. Most models show no significant changes in near-surface mean wind speed until the end of the 21st century. The model ensemble changes range from a 7% decrease to a 6% increase with an ensemble mean decrease of 1 to 2%. Due to model biases, the scale mismatch between model grid and station observations and the missing representation of local winds in the simulations, the changes need to be interpreted with utmost care. Future assessments might lead to major revisions even for the sign of the projected changes, in particular over complex terrain.

KEYWORDS

climatology, future scenarios, homogenisation, model evaluation, near-surface mean wind, reanalysis, regional climate models, Switzerland, trends, wind stilling

1 | INTRODUCTION

Near-surface winds are an important component of the interface between the atmosphere and the land surface. They drive surface and near-surface fluxes of latent and sensible

heat, are of importance for water cycle fluxes and affect local air quality through the transport of pollutants (e.g., Oke, 1987; Stull, 1988; Barmopoulos *et al.*, 2008). Near-surface wind extremes are also a major natural hazard in large parts of the extra-tropics (Shaw *et al.*, 2016), Europe

(Schwierz *et al.*, 2010; Feser *et al.*, 2015) and Switzerland (Stucki *et al.*, 2014; Welker and Martius, 2014). The climatology of near-surface winds, especially their trends in the last decades, has been studied for many regions in the world. In a review of 148 studies, McVicar *et al.* (2012) showed that near-surface wind speeds have decreased in the tropics and mid-latitudes of both hemispheres, whereas at high latitudes of both hemispheres, an increase in wind speed is evident. The widespread decreases of near-surface wind speed are known under the term “stilling” (cf. Roderick *et al.*, 2007). Also, more recent studies show predominantly a stilling in different regions of the world (e.g., Gilliland and Keim, 2018 for a global overview, You *et al.*, 2014 for Tibet, Zha *et al.*, 2017 for China). Explanations for the stilling phenomenon include increasing land surface roughness, circulation changes (e.g., Hadley cell expansion, changes in the storm tracks), measurement artefacts and others (cf. McVicar *et al.*, 2012 for a summary). Vautard *et al.*, (2010) attributed 25–60% of the stilling in the northern mid-latitudes to a growth in vegetation cover and a related increase in surface roughness length and 10–50% to atmospheric circulation changes.

For Switzerland, several studies focus on wind extremes or wind gusts (e.g., Jungo *et al.*, 2002; Goyette *et al.*, 2003; Ceppi *et al.*, 2008; Brönnimann *et al.*, 2012; Welker and Martius, 2014). Beside the studies by Weber and Furger (2001), which determined mean wind patterns in Switzerland, and McVicar *et al.* (2010), who analysed mean wind trends for the period 1960–2006 in Switzerland using non-homogenized data, no recent studies focussing on mean

winds are known to the authors. In this study, the climatology and trends of near-surface mean wind speed in the recent past and the future are presented. In Section 2, the geographical setting and the typical wind systems (Section 2.1), the homogenisation procedure for the observed station data and statistical methods (Section 2.2) and the regional climate model (RCM) and reanalysis data (Section 2.3) are introduced. The climatology and the short-term tendencies of near-surface winds in Switzerland based on a newly homogenized observational data set are presented (Section 3.1) and compared to the long-term evolution of reanalysis data (Section 3.2). Furthermore, the ability of state-of-the-art climate models to represent mean winds and their seasonality in this topographically complex region is assessed (Section 3.3). Future scenarios are analysed, and future trends in mean wind speed are determined in Section 3.4 and some conclusions are drawn in Section 4.

2 | SETTING, DATA AND METHODS

2.1 | Geographical setting and typical wind systems

Switzerland lies in the Northern mid-latitudes, and near-surface winds are strongly determined by the large-scale planetary waves (often westerlies) and the related synoptic-scale flow (eastward passage of fronts, cyclones and anticyclones, e.g., Ahrens, 2012). The complex topography of Switzerland with its three main topographic sub-regions

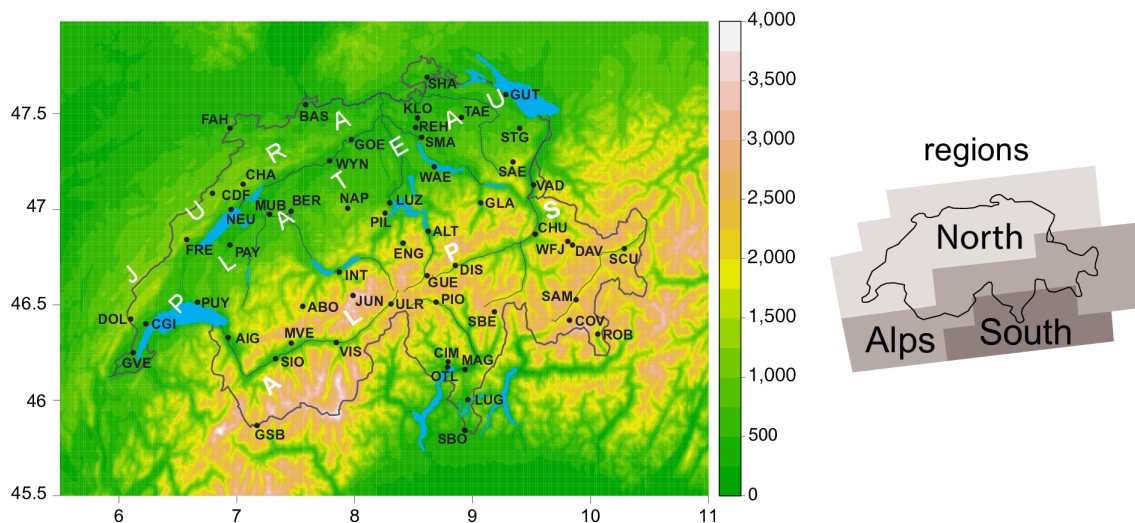


FIGURE 1 Left panel: Map of Switzerland (x-axis: Degrees E, y-axis: Degrees N) showing topography in meters above sea level (shading). The points indicate the locations of wind measurement stations that are part of the automatic monitoring network of MeteoSwiss since the early 1980s and have been used in this study. The three letters are abbreviations of the station names (cf. Table S1). The terms Jura, Plateau and Alps mark the three main distinctive geographical regions of Switzerland. Right panel: The regions used to compute mean wind in future climate scenarios are the same as in the Swiss climate scenario assessment CH2011: North of the Alps, in the Alps and south of the Alps (cf. CH2011, 2011) [Colour figure can be viewed at wileyonlinelibrary.com]

Alps (mountain range, covering ~60% of the Swiss territory), Plateau (hilly terrain, covering ~30% of the Swiss territory) and Jura (mountain range, covering ~10% of the Swiss territory, cf. Figure 1) interacts with the synoptic-scale flow on different scales.

On the Alpine scale, wind systems, such as the frequently occurring westerly winds, are affected by the topography, for example, by horizontal and vertical deflection and increased surface roughness. Fronts are modified (frontal bending), lee cyclones can form, and regional wind systems and gravity waves are triggered (e.g., McGinley, 1982; Kljun *et al.*, 2001). The two most important regional wind systems are (a) the *Föhn*, a wind crossing the main Alpine ridge leading to warm conditions in the lee, affecting many Alpine valleys and sometimes parts of the Plateau (Smith, 1982; Schär *et al.*, 1998; Sprenger *et al.*, 2016) and (b) the *Bise*, an easterly wind most active in the western parts of the Swiss Plateau and an example for deflected flow (Wanner and Furger, 1990; Schär *et al.*, 1998).

On more local scales, thermally driven meso-scale wind systems are induced (e.g., mountain-valley flow, Vergeiner and Dreiseitl, 1987; Whiteman, 1990). The radiative heating over the Alps in the summer season can induce circulations (the so-called Alpine pumping) that extend up to 100 km into the forelands and transport air within the lowest layers towards the Alps (Corsmeier *et al.*, 2003; Weissmann *et al.*, 2005). On the micro scale finally, the near-surface wind conditions can be strongly altered by the surface roughness (e.g., Oke, 1987; Stull, 1988).

Even though numerical models made substantial progress in the last years, they still have problems to provide an accurate representation of near-surface wind speed in complex topography (Cassola and Burlando, 2012; Zhang *et al.*, 2013; Stucki *et al.*, 2016). The reasons include deficiencies in horizontal resolution and physical parameterisations as well problems with initial- and boundary conditions. In order to improve the representation of wind in numerical simulations, we need a better understanding of wind systems in complex topography. The focus of this study in this respect is to give an overview of the observed climatology and trends of near-surface mean wind speed and the ability of state-of-the-art climate models to represent mean winds and their seasonality in Switzerland.

2.2 | Wind measurements

In this study, data of observed near-surface mean wind speed at 54 stations from the automatic monitoring network of MeteoSwiss, the SwissMetNet (SMN, Roulet *et al.*, 2010), are used. The station locations are shown in Figure 1, and more station information is given in Table S1. Wind speed is measured every 10 minutes from which daily and monthly

mean values are computed. The time period considered is 1981–2016 for the comparison with the reanalysis and 1981–2010 for the mean wind climatology and trends. Wind speed is generally measured at 10 m height above ground level, but some deviations from this standard height can occur at some stations (cf. Table S1 for details). The data are not corrected to account for different measurement heights (as, e.g., in Wan *et al.*, 2010) for several reasons. First, it is not straight forward to correct for differences in a general way, especially in complex terrain. Second, an analysis of urban stations that often measure wind on masts on roofs showed that their wind speed values are lying within the range of the variability of the measurements at 10 m of rural stations. Third, our focus is on the assessment of temporal trends and not on the interpretation of the spatial details of wind speed on a fixed height.

2.3 | Homogenisation of station data

Measuring wind speed in a topographically complex region like Switzerland is challenging, and the raw wind data potentially contain considerable inhomogeneities that can generate artificial trends (cf., e.g., Wan *et al.*, 2010; Azorin-Molina *et al.*, 2014). In this study, temporally homogeneous monthly mean near-surface wind speed series are obtained using THOMAS (*Tool for HOMogenisation of Monthly dATA Series*), which was developed at MeteoSwiss (Begert *et al.*, 2003, 2005). The detection of inhomogeneities with this method is a combination of metadata analysis and the use of 12 different homogeneity tests. The homogenisation procedure follows a two-step approach: (a) the detection of inhomogeneities and (b) the calculation of the adjustments. The procedure is able to find and correct the two most frequent types of inhomogeneity in data series, that is, shifts in the mean and linear trends. For each station (hereafter called the candidate series), a reference series is built from nearby stations, which shows the same climatological characteristics as the candidate series and do not contain (any) large inhomogeneities. Metadata are used to find inhomogeneities that affect several stations in the same climatological region at about the same time, because simultaneous shifts in the candidate and the reference series reduce the quality of the homogenisation. The reference series is calculated as a weighted mean from the selected reference stations and using deseasonalised monthly data. The ratio between the candidate and the reference series is used to find shift and trend inhomogeneities. Shift adjustments are calculated by comparing the homogeneous segments before and after the shift with the corresponding segments of a reference series. The significance of the adjustments is then tested using the Wilcoxon rank sum test. Adjustments for trend inhomogeneities are calculated by applying a least-squares fit to the

corresponding part of the ratio series. For the adjustment in THOMAS, metadata information can be additionally included, such as correction factors derived from additional measurements at the site or calibration. This is important for time periods where no reliable reference series can be constructed.

What is the effect of the homogenisation procedure on Swiss wind data using THOMAS? Begert *et al.* (2003) report that on average, a wind series contains an inhomogeneity every 7 years. The main causes for shifts are changes in the instrumentation (67%), calibration (14%) and yearly maintenance (9%). The homogenisation of the wind data starting in 1981 lead to a systematic lowering of the wind speed values in the order of 1 to 4% in the 1980s to mid-1990s compared to the original values. As a consequence, the negative trends in the original series are reduced in the homogenous series.

2.4 | Reanalysis and RCM data

Two data sets of gridded near-surface mean wind data are used in this study: (a) a reanalysis data set to compare the past evolution with station-based measurements and (b) a set of climate model simulations to study model performance and future changes.

The reanalysis data used are the Twentieth Century Reanalysis, version 2c (20CRv2c). It has been chosen because it covers the very long time from 1851 to 2014 (Compo *et al.*, 2011) and it has been used by other wind studies for Switzerland (e.g., Brönnimann *et al.*, 2012; Welker and Martius, 2014). The only variables assimilated in this reanalysis are surface observations of synoptic pressure, monthly sea surface temperature and the sea ice distribution. Near-surface wind speed at 10 m height is analysed in this study. The fields are extracted from the first guess field because they are not available from the reanalysis itself. The data are available on an irregular Gaussian grid (T62) with a horizontal resolution of nearly 200 km. The data set is thus primarily describing the large-scale wind forcing and is not able to represent local winds. The data set consists of 56 ensemble members. The ensemble mean and the spread of the ensemble members are both analysed in this study.

COOrdinated Downscaling EXperiment (CORDEX) data are used to investigate potential impact of future climate change on the mean wind speed in Switzerland. CORDEX is an initiative to coordinate regional downscaling of multiple general circulation models (GCMs) from the Coupled Model Intercomparison Project Phase 5 (CMIP5). For the European domain (EURO-CORDEX), a set of RCMs is provided at two different spatial resolutions: a coarser resolution of 0.44° (EUR-44, 50 km) and a finer resolution of 0.11° (EUR-11, 12.5 km). Only near-surface wind speed at 10 m

height is considered, which is interpolated from other model levels and hence a diagnostic variable. Seventy-five model simulations for the three emission scenarios RCP2.6, RCP4.5 and RCP8.5 are used in this study, which are listed in Table S2. All published simulations are considered, also those for which a “warning” has been published on the EURO-CORDEX errata-page (e.g., simulations based on the CNRM-CM5 GCM) and the ones that do not run until the year 2099. Details about the parameterisation of each RCM are summarized in Kotlarski *et al.* (2014). Note that for some trend analyses only RCP4.5 model simulations are displayed because the differences to other scenarios do not exceed $\pm 0.1 \text{ ms}^{-1}$.

2.5 | Statistical methods

The Theil–Sen estimator is used for the calculation of linear trends (Theil, 1950; Sen, 1968). It is calculated as the median of all pairwise slopes. The Theil–Sen estimator is more robust against outliers than the ordinary least squares method. The non-parametric Mann–Kendall trend test is used to detect if time series follow a monotonic trend (Mann, 1945; Kendall, 1955). The Bonferroni–Holm method is intended to deal with familywise error rates for multiple hypothesis tests (e.g., testing spatially distributed stations), because the more hypotheses are checked, the higher the probability of a type I error (Holm, 1979). Therefore, it adjusts the rejection criteria of each of the individual hypotheses. For the relative trends (Figure 2d), the Bonferroni–Holm method is used and compared with the less strict Mann–Kendall significance applied to the absolute trends (Figure 2c).

3 | RESULTS

3.1 | Climatology of mean wind 1981–2010

3.1.1 | Wind speed

The yearly mean wind speeds in the period 1981–2010 are lowest at stations in inner Alpine valleys (e.g., Disentis and Scuol) and at low elevations of southern Switzerland (canton Ticino) with values between 0.9 and 1.6 ms^{-1} (Table S1; Figure 2a). Slightly higher values are found on the Swiss Plateau with typical mean wind speeds between 1.4 and 2.5 ms^{-1} . Note that wind speed values on roofs in cities (e.g., Zürich, Wädenswil or Luzern) with a measurement height of almost 30 to over 40 m above ground are within the range of the values of rural stations. This indicates that the higher measurement height is compensating well the decreased wind speed caused by the increased surface roughness in cities. The yearly mean wind speeds in the Alpine valleys show a larger variability with values between

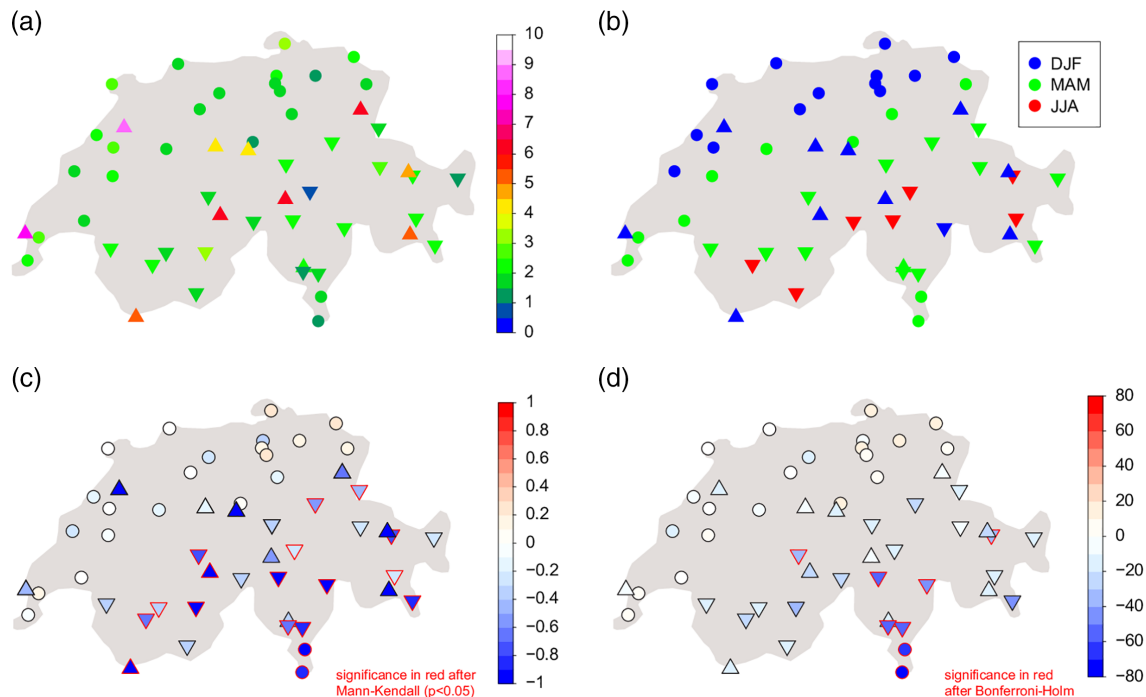


FIGURE 2 Wind climatology for the period 1981–2010: (a) yearly mean wind in ms^{-1} (colours); (b) season with the highest seasonal mean wind; (c) absolute trends in ms^{-1} per century, the red border of the symbols indicates if the trend is significant on the 0.05 level using the Mann–Kendall trend test; (d) relative trends in percent per century, the red border shows significant trends on the 0.05 level using the more strict Bonferroni–Holm test. The triangles pointing upward mark mountain stations, triangles pointing downward valley stations and circles stations in other terrain [Colour figure can be viewed at wileyonlinelibrary.com]

0.9 and 3.2 ms^{-1} . The higher values are mainly related to local phenomena, such as thermally driven valley winds. The highest mean wind speeds are observed at mountain peaks. However, they are not only influenced by the height above sea level (asl). In the Jura mountains, the mean wind speed reach values of up to 8.6 ms^{-1} on the Chasseral ($1,613 \text{ m asl}$) and 7.8 ms^{-1} on La Dôle ($1,683 \text{ m asl}$). These wind speeds are higher than the mean winds on much higher Alpine mountain peaks with values between 4.8 ms^{-1} on the Weissfluhjoch (WFJ) ($2,701 \text{ m asl}$) and 6.3 ms^{-1} on the Jungfrauoch ($3,581 \text{ m asl}$). The high values on the Jura mountains are partly linked to the fact that on the Jura summits the Bise is often active in times with weak wind situations on Alpine summits. An additional effect could be the increased effective surface roughness in the Alps compared to the hillier and comparatively smooth terrain of the Jura.

3.1.2 | Seasonality

The complexity of the wind regime in Switzerland is not only reflected in the mean wind speed but also in its seasonality. Figure 2b shows the season with strongest seasonal mean winds in the period 1981–2010 for every station. Most stations in northern Switzerland and on mountain peaks have a maximum during winter (December, January, February). The main driver during this season is the large-scale flow

(i.e., the westerlies). In the southern Alps and many (pre-) alpine valleys, strongest winds occur in spring (March, April or May). In most inner Alpine valleys, the seasonal mean wind maximum occurs in summer (June, July, August). Especially in the Alpine valleys and in the southern Alps, the wind maximum in spring and summer are due to thermally driven orographic wind systems (mountain-valley winds), thunderstorms and especially in spring also due to Föhn events (Gutermann *et al.*, 2012; Cetti *et al.*, 2015). It is interesting that there are no stations that show a maximum in autumn (September, October, November). For most stations, the weakest mean winds are found in summer or autumn. Only for stations in Alpine valleys, the minimum is found in winter (not shown).

3.1.3 | Short-term tendencies

The availability of countrywide homogenized station data opens the possibility to compute trends. Unfortunately, the mean wind series are not very long, and only short-term tendencies can be computed, which can then be compared with long-term reanalysis data. The absolute tendencies for the period 1981–2010 range between a wind speed decline of -1.25 ms^{-1} per century (on the Jungfrauoch and Chasseral) and a slight increase of $+0.24 \text{ ms}^{-1}$ per century (Güttingen; Table S1; Figure 2c, d). Negative tendencies are present at

most Swiss stations. Slightly positive or no tendencies are found in the north-eastern Swiss Plateau. The negative tendencies are more pronounced in the Jura, Alps and southern Alps. The relative tendencies are largest in southern Switzerland, especially in the lowland of Ticino with declines of 50% or more. On the Swiss Plateau on the other hand, the relative tendencies are small with values between -18.5 and $+11.1\%$ per century. The tendencies are significant (Mann–Kendall trend test at the 0.05 level) at many stations in the Alps and the southern Alps (Figure 2c). If the stricter Bonferroni–Holm method is used, the short-term tendencies are still significant at the 0.05 level in southern Switzerland, Davos and Interlaken (Figure 2d). Note, however, that there is still a chance that these tendencies are purely caused by internal or decadal variability and they need to be put into perspective with longer series.

3.2 | Comparison with century-scale reanalysis (20CRv2c)

In order to put the recent tendencies into a longer term perspective, a comparison with the decadal variability in the 20CRv2c reanalysis is performed. The annual mean of the 10 m wind speed of observations at 27 stations north of the Alps are compared with the most representative grid point of the 20CRv2c data set. Because of the coarse resolution of 20CRv2c, the selected grid point is located north of Switzerland at $48.6^{\circ}\text{N}/7.5^{\circ}\text{E}$. Stations in and south of the Alps are excluded in this analysis, because it cannot be expected that 20CRv2c is capable to reproduce the wind speed in

mountainous terrain. For each station, the values of the annual mean are normalized to zero mean and one standard deviation for the period 1981–2014. Subsequently, the mean of the normalized values over all 27 stations is calculated. The normalization is also performed to the ensemble mean of 20CRv2c for the same time period. The ensemble mean of 20CRv2c and the mean of the observations are in a good agreement with a Pearson correlation coefficient of $r = 0.745$ (Figure 3), and both data sets show an increase until the late 1990s and a subsequent decrease. Note that if the first three years 1981–1983 are excluded, r increases even to 0.836. This could indicate problems with the wind measurements in the early 1980s possibly in conjunction with the introduction of the first generation of the automated measurement network. The mean absolute wind speed in 20CRv2c is 3.5 ms^{-1} and substantially higher than that of the observations with 2.5 ms^{-1} . The reason for this bias has not been investigated in detail but could be linked to the fact that the lowest model (0.995 sigma) level corresponds to approximately 42 m above ground.

The 1981–2010 values lie well within the range of 20CRv2c long-term variability, and there is no indication of a general long-term decline in 20CRv2c. There is an episode of increasing mean winds in 20CRv2c from about 1950 to the late 1980s. This is qualitatively in line with results from McVicar *et al.* (2010) who found increasing mean winds for the period 1960–1983. We take this as a possible indication that the decrease of mean wind speed in the period 1981–2010 could be easily caused by natural decadal variability. However, it cannot be ruled out per se that other

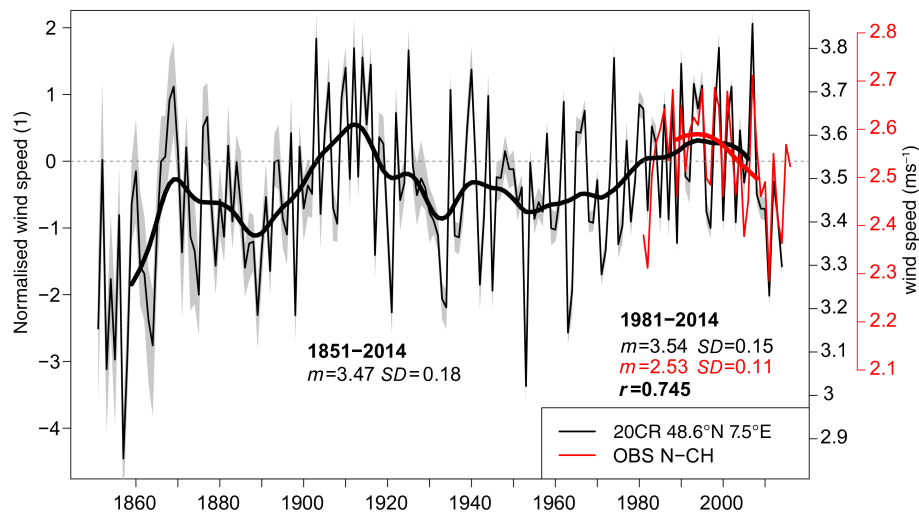


FIGURE 3 Annual mean wind speed of 20CRv2c ensemble mean (thin black line; $48.57^{\circ}\text{N}/7.5^{\circ}\text{E}$) and an average of homogenized observations north of the Alps (thin red line). The normalization to zero mean and unit standard deviation (left axis) is performed for the period 1981–2014 for both quantities. The thick lines are Gaussian smoothed over a 20-year period. The grey shaded area shows the spread between the minimum and maximum of the 20CRv2c ensemble members. The y-axes on the right side show absolute wind speed for comparison (20CRv2c in black, homogenized observations in red). m is the mean, and SD is the standard deviation of the absolute values for the specified time period. r is the Pearson correlation coefficient between 20CRv2c and homogenized observations [Colour figure can be viewed at wileyonlinelibrary.com]

factors than natural variability (e.g., a systematic increase in surface roughness or changes in the global circulation due to climate change) are also partly responsible for the decrease of winds in the recent past. Earlier studies found good agreement of the decadal variability of peak winds between 20CRv2c and observations (Brönnimann *et al.*, 2012; Welker and Martius, 2014). It has to be noted, though, that the observational input in 20CRv2c is very sparse in the 19th century, especially before the 1870s and the very low values at the beginning of the 20CRv2c series could be an artefact.

3.3 | RCM evaluation

In order to assess the confidence in RCM-based scenario simulations, an evaluation of the models' ability to represent mean winds and some aspects of the seasonality in the Alpine region is helpful. However, a fair comparison between observations and model output is difficult to achieve. Ideally, the gridded CORDEX RCM data would be

compared with gridded observational data on the same grid. Since there is no reliable gridded observational data set available, the model data are evaluated against station-based wind observations in the reference period 1981–2010. This considerable scale-gap needs to be kept in mind for this evaluation, especially in complex terrain.

In Figure 4, the absolute biases (value of the closest model grid point minus observations) of the 30-year-mean wind speed are shown for different stations. Absolute biases highly depend on the RCM (same colour). The driving GCM and the model resolution (EUR-11 [bold] vs. EUR-44) seem to have only minor effects on the biases. Most models underestimate mean winds in the Alps. CLMcom-CCLM, HMS-ALADIN52 (not shown), KNMI-RACMO22E clearly underestimate the wind speed on mountain summits. The underestimation is smaller for DMI-HIRHAM5, ICTP-RegCM4-3 and SMHI-RCA4. For the latter model, some model simulations slightly overestimate winds at the WFJ.

All models clearly underestimate winds in the Jura mountains. In the lower regions (Alpine valleys, Plateau and

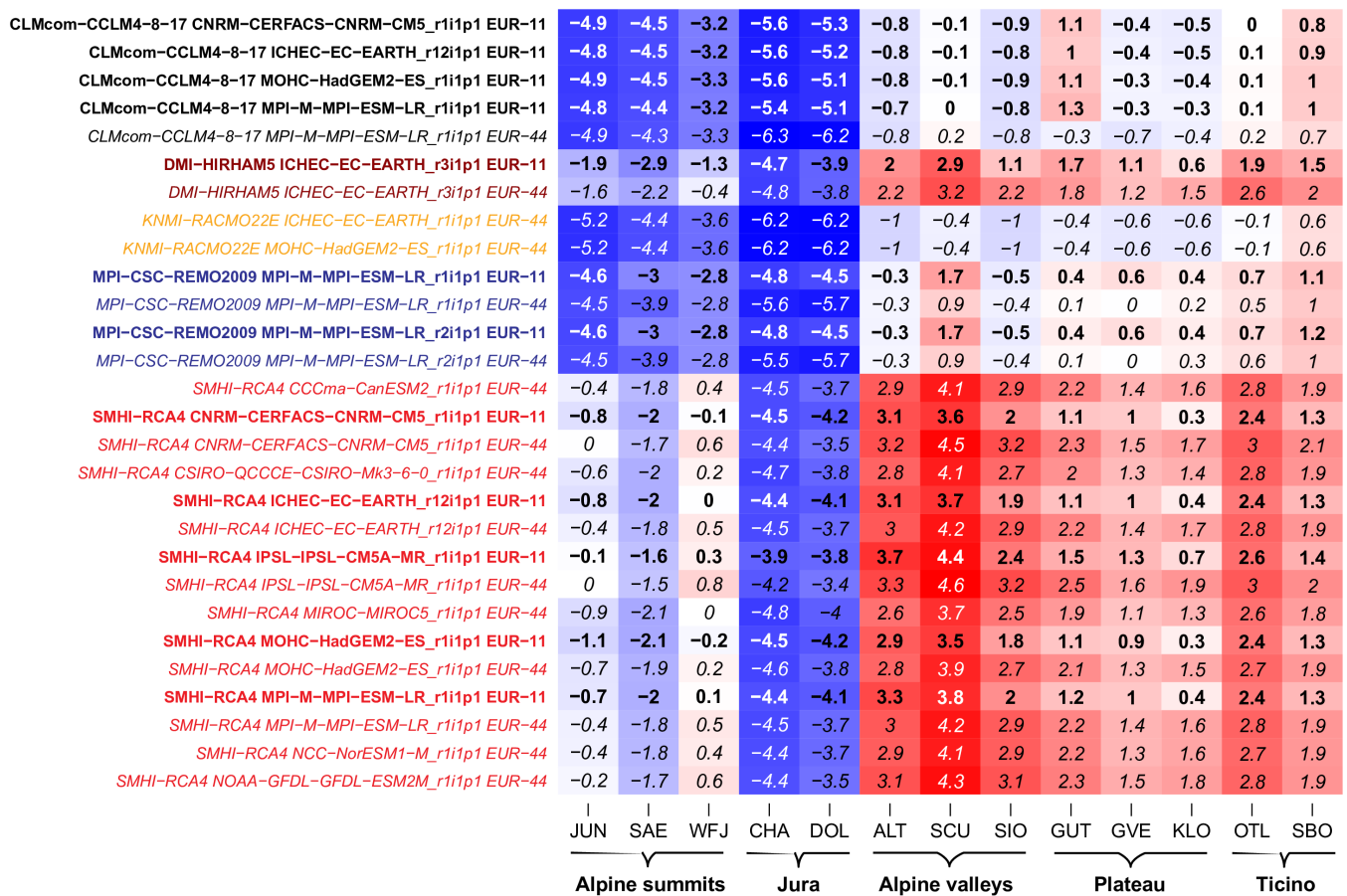


FIGURE 4 Absolute bias (model minus observations) of the mean wind in period 1981–2010 for the CORDEX RCP4.5 model simulations (rows) for selected stations (columns). The stations are clustered by region (Alpine summits, Jura, Alpine valleys, Plateau and Ticino). The simulations are sorted by RCM (black: CLMcom-CCLM4; brown: DMI-HIRHAM5; orange: KNMI-RACMO22E, blue: MPI-CSC-REMO2009, red: SMHIRCA4). The EUR-11 simulations are bold and the EUR-44 simulations are italic. The model is evaluated at the closest grid point relative to the meteorological station. Blueish (reddish) colours represent negative (positive) biases [Colour figure can be viewed at wileyonlinelibrary.com]

Ticino) DMI-HIRHAM5, ICTP-RegCM4-3 (not shown) and SMHI-RCA4 overestimate the wind speed considerably. For these models, the overestimation is more pronounced for stations in Alpine valleys than on the Plateau. In contrast, CLMcom-CCLM, HMS-ALADIN52 (not shown), KNMI-RACMO22E and MPI-CSC-REMO2009 show smaller biases in the lower regions (Alpine valleys, Plateau and Ticino). CLMcom-CCLM, HMS-ALADIN52 (not shown) and KNMI-RACMO22E somewhat underestimate the winds at most grid points, whereas MPI-CSC-REMO2009 shows a weak overestimation at a majority of the stations.

The spatial representation of the 30-year-mean wind in the period 1981–2010 is depicted for a selection of model simulations in Figure 5. The general spatial pattern of the same driving RCMs correlates strongly between the two different resolutions and also between different driving GCMs (not shown). Some differences seem to be mainly related to

the different representation of the topography due to the different model resolution. However, considerable differences exist between different RCMs especially in the Alps, where the mean wind speeds range from about 1 to 2 ms^{-1} (e.g., CLMcom-CCLM) to more than 5 ms^{-1} (e.g., SMHI-RCA4). In some models, wind speed tends to decrease with increasing altitude (e.g., CLMcom-CCLM, MPI-CSC-REMO2009, Figure 5a-d). In other models, wind speed increases with increasing altitude (e.g., DMI-HIRHAM5, SMHI-RCA4, Figures 5e-h).

An important feature of wind climatology is a good representation of the seasonal cycle. Figure 6 shows the season with maximum wind speed for observations and models. The spatial patterns seem to be mainly determined by the driving GCM (rows in Figure 6). As in the observations (repeated from Figure 2b), most models show a maximum in winter at most stations. A small number of simulations show

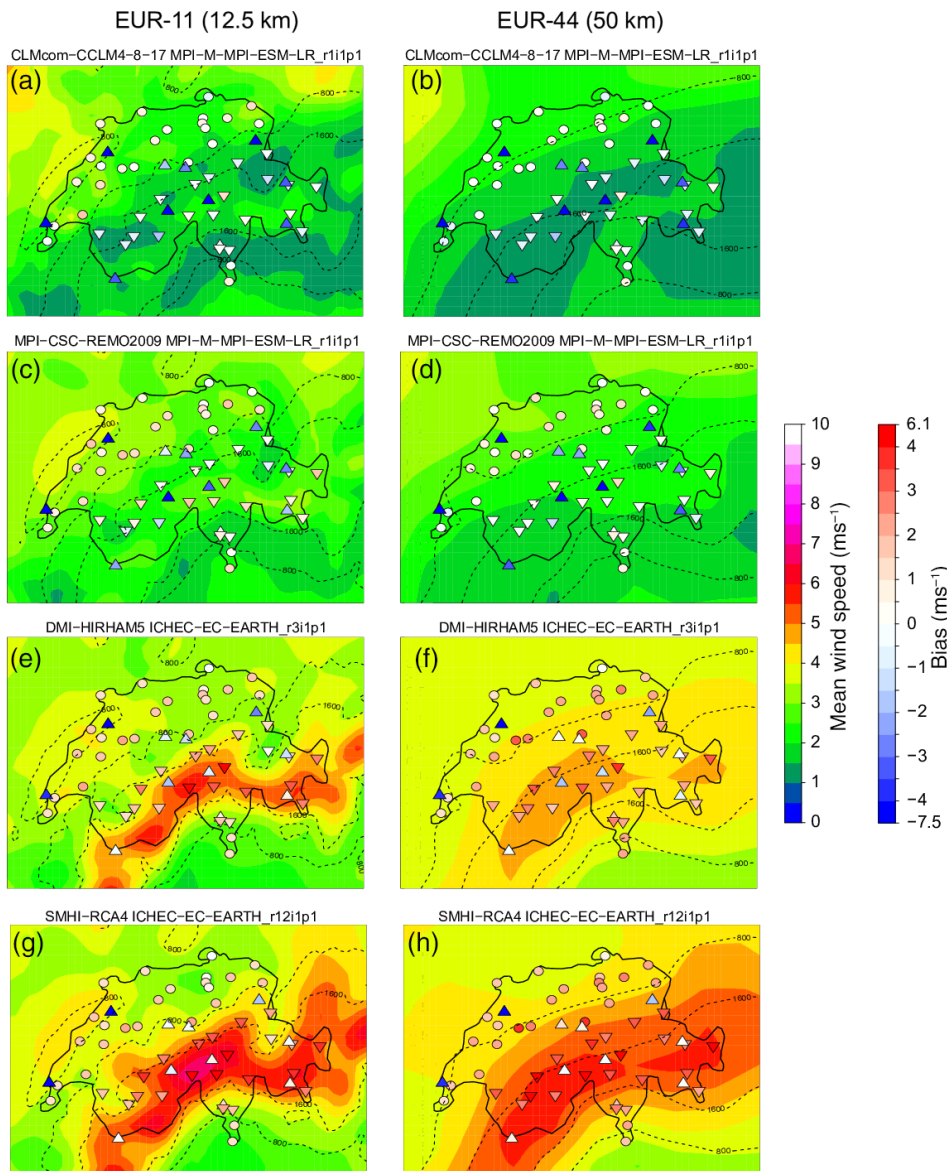


FIGURE 5 30-year-mean near-surface mean wind fields (colour shading, left colour bar in ms^{-1}) and bias (model minus observation at stations [symbols as in Figure 2], right colour bar in ms^{-1}) for a selection of simulations ((a, b) CCLM MPI-ESM-LR, (c, d) REMO2009 MPI-ESM-LR, (e, f) HIRHAM5 EC-EARTH, (g, h) RCA4 EC-EARTH) in the period 1981–2010. Each row shows the same RCM, but with different resolution. EUR-11 simulations are shown in the left column, EUR-44 simulations in the right one. The black dashed lines represent the model topography in both resolutions respectively (isolines at 800 and 1,600 m above sea level) [Colour figure can be viewed at wileyonlinelibrary.com]

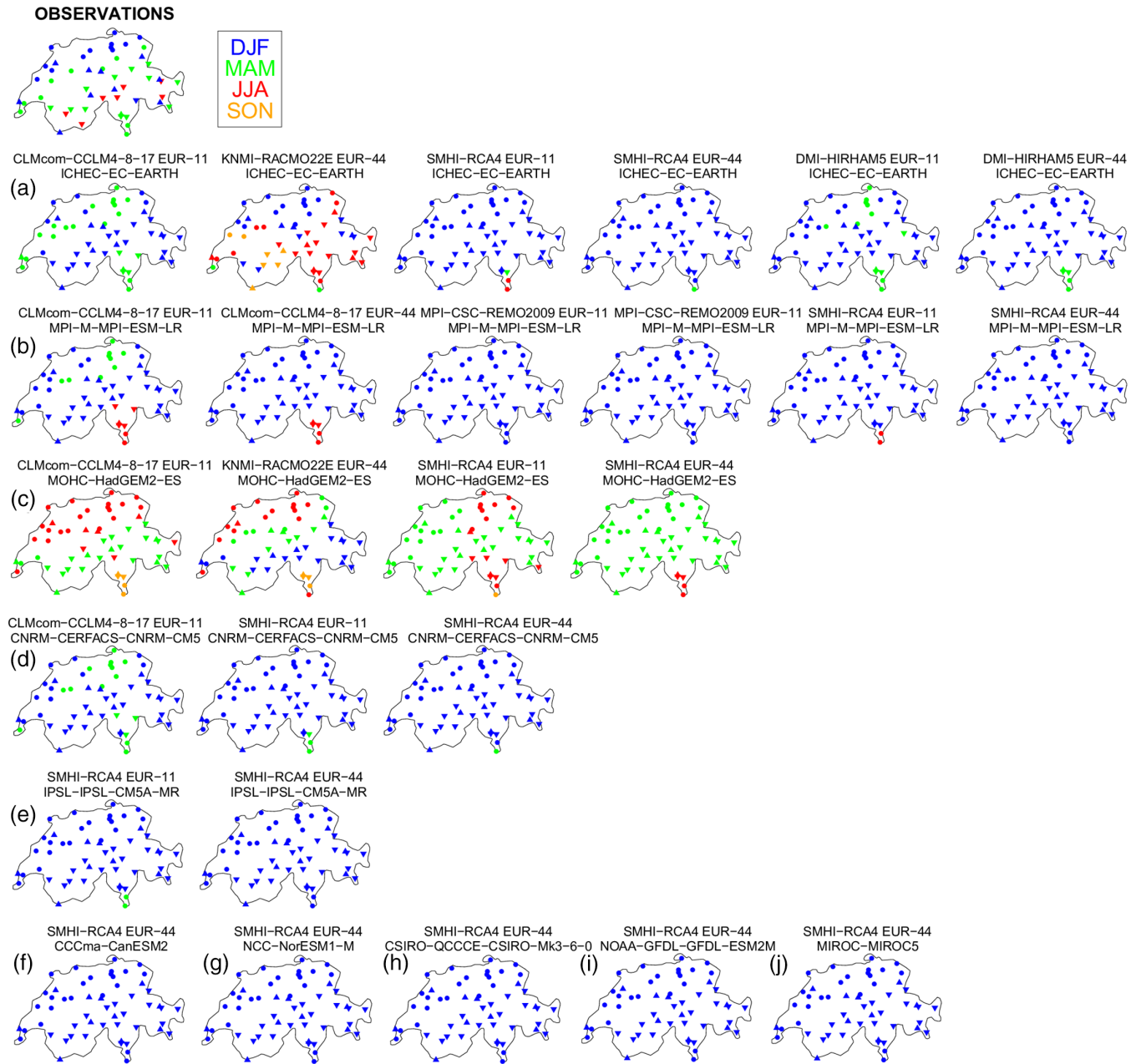


FIGURE 6 Season with maximum mean wind speed (period 1981–2010) for the observations (top left panel) and for the CORDEX RCM simulations (other panels). The models are evaluated at the closest grid point relative to the meteorological station. Simulations are sorted by GCM ((a) EC-EARTH, (b) MPI-ESM-LR, (c) HadGEM2-ES, (d) CNRM-CM5, (e) IPSL-CM5A-MR, (f) CanESM2, (g) NorESM1-M, (h) CSIRO-Mk3-6-0, (i) GFDL-ESM2M, (j) MIROC5). Where EUR-11 and EUR-44 simulations are available for the same GCM, the EUR-11 simulation is always shown first (i.e., left) of the EUR-44 simulation [Colour figure can be viewed at wileyonlinelibrary.com]

a maximum in summer predominantly on the Plateau and in the Jura. The observed maximum in spring and summer in mountain valleys is not found in the models. The season of the minimum mean wind speed has also been analysed (not shown). In the observations, summer and autumn are the dominant season for the minimum, except for the stations in mountain valleys, where the minimum is found in winter. In comparison, most model simulations also have the minimum in summer or autumn. However, none of the model

simulations reproduces the winter minimum in mountain valleys. The difference between GCM-RCM model simulations where both resolutions (EUR-11 and EUR-44) are available is rather small. Also note that the higher resolution EUR-11 simulations do not show clearly better results than the low-resolution EUR-44 simulations. The reasons for the differences between observations and model simulations have not been investigated in detail but the above results are a good indication that an insufficient representation of local

wind systems, such as thermally driven mountain-valley winds, Föhn, Bise, convection and thunderstorms, could play an important role here.

3.4 | Mean wind in future climate scenarios

In this section, future scenarios of 30-year-mean wind speed in the 75 simulation EURO-CORDEX model ensemble are presented for Switzerland. Figure 7 (top row) shows the evolution of the mean wind speed for the three different CH2011 regions in Switzerland for all emission scenarios (cf. CH2011, 2011). The absolute values depend strongly on the RCM (different colours). The differences between the RCMs are largest in the Alps (mean wind speed values range between less than 1 and almost 6 ms^{-1}) and smaller north (range 1 to 5 ms^{-1}) and south (range 1 to 4 ms^{-1}) of the Alps. The mean wind speed is lower at the southern side of the Alps compared to the northern side. Also note that the temporal changes of a particular model simulation are much smaller than the differences between different RCMs.

In the bottom row, the absolute change in ms^{-1} of each model simulation relative to the reference period 1981–2010 is presented. The majority of simulations show a slight

tendency for a decrease of the 30-year-mean wind speed in all three regions until the end of the 21st century, but some model simulations exhibit a very weak tendency of an increase in wind speed in all regions. Note that the changes are small and mostly not statistically significant. For the period 2070–2099, the mean changes for the “North” are -0.04 ms^{-1} (–1.2%) with a range from -0.18 to $+0.08 \text{ ms}^{-1}$ (–5.5 to +3.9%). The mean changes for the “Alps” are -0.07 ms^{-1} (–1.7%) with a range from -0.33 to $+0.07 \text{ ms}^{-1}$ (–6.6 to +6%). In the “South,” the mean changes are -0.05 ms^{-1} (–1.7%) with a range from -0.21 to $+0.07 \text{ ms}^{-1}$ (–6 to +5%). The numbers are in broad agreement with the results of Kjellström *et al.* (2018), when inspecting their maps of Europe over Switzerland. The largest decreases are found for SMHI-RCA4 simulations. There is a tendency that the models with lower mean wind speeds (e.g., CLMcom-CCLM4-8-17) also show smaller absolute trends and a smaller spread. The opposite is the case for models with higher wind speeds (e.g., SMHI-RCA4). The differences between the scenarios are small. There is a weak tendency for larger changes in the high emission scenario RCP8.5 (red dot in Figure 7) compared to the lower emission scenarios RCP4.5 (orange dot) and RCP2.6 (green dot).

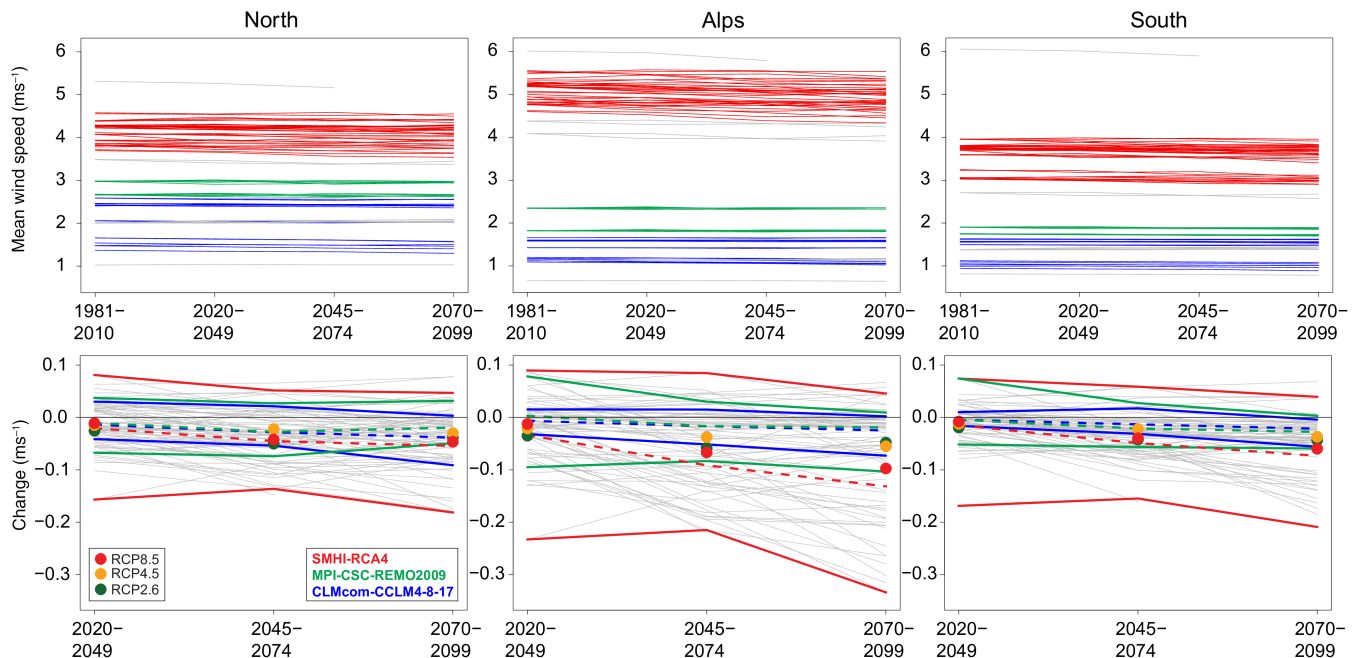


FIGURE 7 Evolution of the RCM's near-surface mean wind speed averaged over 30-year periods and for the three Swiss regions “North,” “Alps” and “South” (columns) defined in Figure 1 for 75 simulations of the EURO-CORDEX model ensemble including RCP2.6, RCP4.5 and RCP8.5 scenarios. Top row: Absolute values in ms^{-1} for the mean of reference period 1981–2010, the periods 2020–2049, 2045–2074 and 2070–2099. The colours represent identical RCMs (red = SMHI-RCA4; brown = MPI-CSC-REMO2009; blue = CLMcom-CCLM4-8-17; grey = others). Bottom row: Absolute changes in ms^{-1} relative to the reference period 1981–2010. The coloured lines show the maximum and minimum values (solid lines) and the mean value (dashed lines) for the three coloured RCMs in the top row (including all representative concentration pathways (RCPs)). The dots show the average changes over all RCP2.6 (green, 11 simulations), RCP4.5 (orange, 28 simulations) and RCP8.5 (red, 36 simulations) simulations. Also simulation that do not cover the whole time period are shown [Colour figure can be viewed at wileyonlinelibrary.com]

Note that the number of model simulations is different for the different scenarios and parts of the differences could arise from the different sample size.

4 | DISCUSSION AND CONCLUSIONS

In this paper, we present an analysis of the near-surface mean wind evolution in Switzerland in the recent past and the future using several data sources. The station observations between 1981 and 2010 show significant decreases in the Alps and on the southern Alpine slope. This is in agreement with an earlier result by McVicar *et al.* (2010) and most regions in the mid-latitudes (see, e.g., McVicar *et al.*, 2012). A comparison with the long-term evolution in the 20CRv2c reanalysis shows that station observations and the reanalysis agree very well in the period 1981–2014. Also, the 20CRv2c tendency for increasing mean winds from about 1950 to the late 1980s is qualitatively in line with observations (cf. McVicar *et al.*, 2010). The 20CRv2c long-term evolution since the mid-19th century indicates that the recent negative tendency lies well within the decadal variability and the mean wind recovered somewhat after the year 2010. Since 20CRv2c does not include changes in surface roughness, this is one indication that changes in surface roughness are probably not the dominant driver of the recent trends in Swiss mean wind. However, since not all possible factors (e.g., a comparison with upper-air winds) have been analysed in this study, it cannot be ruled out that changes are partly related to factors often mentioned in connection with the wind stalling phenomenon.

The RCM validation exercise (based on a station and nearest grid point comparison) shows that climate modelling of near-surface winds in complex topography with grid resolutions larger than 10 km remains a challenge. The largest absolute biases of the wind speed are present over mountainous terrain. All models show large absolute biases in the Jura mountains and some models show large biases in the Alps. The absolute biases are highly correlated with the underlying RCM. The driving GCMs and the model resolution (EUR 11 or EUR-44) seem to have only minor effects on the biases. The differences between different RCMs are most probably a result of different model parameterisations for near-surface wind speed. This would also explain the small differences of the biases for different model simulations of the same RCM. The two considered model resolutions have a similar effect on the representation of the mean wind in Alpine terrain. The 12.5 km resolution in EUR-11 is not sufficient to represent near-surface winds in complex topography markedly better than with a resolution of 50 km in the EUR-44 simulations.

The RCMs are mostly able to represent the seasonality of the large-scale forcing coming from the GCMs

(maximum mean wind speed in winter and minimum in summer) but miss important details in complex terrain. The main reason seems to be the inadequate representation of thermally driven orographic wind system (mountain-valley winds) and possibly also Föhn and Bise. Again, this indicates that the applied model resolution may not be sufficient to represent relatively small-scale mountain-valley wind systems and further downscaling (either dynamical or statistical) may be necessary to show a realistic seasonality in complex topography. Upcoming convection resolving models on the kilometre scale (cf., e.g., Leutwyler *et al.*, 2017; Fuhrer *et al.*, 2018) may significantly improve small-scale wind effects, especially in the summer season.

The future scenarios of near-surface wind speed in Switzerland based on 75 EURO-CORDEX simulations show only weak (and mostly insignificant) change signals. For the end of the 21st century (2070–2099), the model ensemble changes range from a 7% decrease to a 6% increase with an ensemble mean decrease of about 1 to 2%. Taking into consideration that models have difficulties with the representation of near-surface winds in complex topography, the trend signals in the climate models should be interpreted very carefully. It is possible that changes in the wind-relevant parameterisation or in the model resolution will lead to major changes in the results for future assessments, in particular over complex terrain such as in the Alps.

ACKNOWLEDGEMENTS

M.G. was supported by the Swiss National Centre for Climate Services (NCCS). Support for the Twentieth Century Reanalysis Project dataset is provided by the U.S. Department of Energy, Office of Science Innovative and Novel Computational Impact on Theory and Experiment program, and Office of Biological and Environmental Research, and by the National Oceanic and Atmospheric Administration Climate Program Office. The authors thank the coordination and participating institutes of the EURO-CORDEX initiative for their efforts to make the simulation data available for analysis.

ORCID

Simon C. Scherrer  <https://orcid.org/0000-0002-5040-0470>
Michael Begert  <https://orcid.org/0000-0002-9569-6842>

REFERENCES

- Ahrens, C.D. (2012) *Meteorology Today: An Introduction to Weather, Climate, and the Environment*. Belmont, CA: Cengage Learning.
- Azorin-Molina, C., Vicente-Serrano, S.M., McVicar, T.R., Jerez, S., Sanchez-Lorenzo, A., López-Moreno, J., Revuelto, J., Trigo, R.M.,

- Lopez-Bustins, J.A. and Espírito-Santo, F. (2014) Homogenization and assessment of observed near-surface wind speed trends over Spain and Portugal, 1961–2011. *Journal of Climate*, 27, 3692–3712. <https://doi.org/10.1175/JCLI-D-13-00652.1>.
- Barnpadimos, I., Hueglin, C., Keller, J., Henne, S. and Prévôt, A.S.H. (2008) Influence of meteorology on PM10 trends and variability in Switzerland from 1991 to 2008. *Atmospheric Chemistry and Physics*, 11, 1813–1835. <https://doi.org/10.5194/acp-11-1813-2011>.
- Begert, M., Schlegel, T. and Kirchofer, W. (2005) Homogeneous temperature and precipitation series of Switzerland from 1864 to 2000. *International Journal of Climatology*, 25, 65–80. <https://doi.org/10.1002/joc.1118>.
- Begert, M., Seiz, G., Schlegel, T., Musa, M., Baudraz, G. and Moesch, M. (2003) *Homogenisierung von Klimamessreihen der Schweiz und Bestimmung der Normwerte 1961–1990. Schlussbericht des Projektes NORM90*. Veröffentlichungen der MeteoSchweiz 67. Zürich: Bundesamt für Meteorologie und Klimatologie MeteoSchweiz. (in German)
- Brönnimann, S., Martius, O., von Waldow, H., Welker, C., Luterbacher, J., Compo, G.P., Sardeshmukh, P.D. and Usbeck, T. (2012) Extreme winds at northern mid-latitudes since 1871. *Meteorologische Zeitschrift*, 21, 13–27. <https://doi.org/10.1127/0941-2948/2012/0337>.
- Cassola, F. and Burlando, M. (2012) Wind speed and wind energy forecast through Kalman filtering of numerical weather prediction model output. *Applied Energy*, 99, 154–166. <https://doi.org/10.1016/j.apenergy.2012.03.054>.
- Ceppi, P., Della-Marta, P. M. and Appenzeller, C. (2008) *Extreme value analysis of wind speed observations over Switzerland*. Arbeitsberichte der MeteoSchweiz 219. Zürich: Bundesmat für Meteorologie und Klimatologie.
- Cetti, C., Buzzi, B. and Sprenger, M. (2015) *Climatology of Alpine north foehn*. Scientific Report MeteoSwiss 100. Zürich: MeteoSwiss.
- CH2011. (2011) *Swiss Climate Change Scenarios CH2011*. Zurich: C2SM, MeteoSwiss, ETH, NCCR Climate, and OcCC.
- Compo, G.P., Whitaker, J.S., Sardeshmukh, P.D., Matsui, N., Allan, R. J., Yin, X., Gleason, B.E., Vose, R.S., Rutledge, G., Bessemoulin, P., Brönnimann, S., Brunet, M., Crouthamel, R.I., Grant, A.N., Groisman, P.Y., Jones, P.D., Kruk, M.C., Kruger, A. C., Marshall, G.J., Maugeri, M., Mok, H.Y., Nordli, Ø., Ross, T.F., Trigo, R.M., Wang, X.L., Woodruff, S.D. and Worley, S.J. (2011) The twentieth century reanalysis project. *Quarterly Journal of the Royal Meteorological Society*, 137, 1–28. <https://doi.org/10.1002/qj.776>.
- Corsmeier, U., Kottmeier, C., Winkler, P., Lugauer, M., Reitebuch, O. and Drobinski, P. (2003) Flow modification and mesoscale transport caused by Alpine Pumping: A VERTIKATOR case study. In: *Proceedings of International Conference on Alpine Meteorology and Mesoscale Alpine Project Meeting* (Brig), Vol. A. Brig: International Conference on Alpine Meteorology, pp. 138–140.
- Feser, F., Barcikowska, M., Krueger, O., Schenk, F., Weisse, R. and Xia, L. (2015) Storminess over the North Atlantic and northwestern Europe—a review. *Quarterly Journal of the Royal Meteorological Society*, 141, 350–382. <https://doi.org/10.1002/qj.2364>.
- Fuhrer, O., Chadha, T., Hoefler, T., Kwasniewski, G., Lapillonne, X., Leutwyler, D., Lüthi, D., Osuna, C., Schär, C., Schulthess, T.C. and Vogt, H. (2018) Near-global climate simulation at 1km resolution: establishing a performance baseline on 4888 GPUs with COSMO 5.0. *Geoscientific Model Development*, 11, 1665–1681. <https://doi.org/10.5194/gmd-11-1665-2018>.
- Gilliland, J.M. and Keim, B.D. (2018) Surface wind speed: trend and climatology of Brazil from 1980–2014. *International Journal of Climatology*, 38, 1060–1073. <https://doi.org/10.1002/joc.5237>.
- Goyette, S., Brasseur, O. and Beniston, M. (2003) Application of a new wind gust parameterization: multiscale case studies performed with the Canadian regional climate model. *Journal of Geophysical Research*, 108, 4374. <https://doi.org/10.1029/2002JD002646>.
- Gutermann, T., Dürr, B., Richner, H. and Bader, S. (2012) *Föhnklimatologie Altdorf: die lange Reihe (1864–2008) und ihre Weiterführung*. Vergleich mit anderen Stationen, Fachbericht MeteoSchweiz 241. Zürich: Bundesamt für Meteorologie und Klimatologie MeteoSchweiz. (in German)
- Holm, S. (1979) A simple sequentially rejective multiple test procedure. *Scandinavian Journal of Statistics*, 6, 65–70.
- Jungo, P., Goyette, S. and Beniston, M. (2002) Daily wind gust speed probabilities over Switzerland according to three types of synoptic circulation. *International Journal of Climatology*, 22, 485–499. <https://doi.org/10.1002/joc.741>.
- Kendall, M.G. (1955) *Rank Correlation Methods*. New York, NY: Hafner Publishing Co.
- Kjellström, E., Nikulin, G., Strandberg, G., Christensen, O.B., Jacob, D., Keuler, K., Lenderink, G., van Meijgaard, E., Schär, C., Somot, S., Sørland, S.L., Teichmann, C. and Vautard, R. (2018) European climate change at global mean temperature increases of 1.5 and 2 °C above pre-industrial conditions as simulated by the EURO-CORDEX regional climate models. *Earth System Dynamics*, 9, 459–478. <https://doi.org/10.5194/esd-9-459-2018>.
- Kljun, N., Sprenger, M. and Schär, C. (2001) Frontal modification and lee cyclogenesis in the Alps: a case study using the ALPEX reanalysis data set. *Meteorology and Atmospheric Physics*, 78, 89–105. <https://doi.org/10.1007/s007030170008>.
- Kotlarski, S., Keuler, K., Christensen, O.B., Colette, A., Déqué, M., Gobiet, A., Goergen, K., Jacob, D., Lüthi, D., van Meijgaard, E., Nikulin, G., Schär, C., Teichmann, C., Vautard, R., Warrach-Sagi, K. and Wulfmeyer, V. (2014) Regional climate modeling on European scales: a joint standard evaluation of the EURO-CORDEX RCM ensemble. *Geoscientific Model Development*, 7, 1297–1333. <https://doi.org/10.5194/gmd-7-1297-2014>.
- Leutwyler, D., Lüthi, D., Ban, N., Fuhrer, O. and Schär, C. (2017) Evaluation of the convection-resolving climate modeling approach on continental scales. *Journal of Geophysical Research*, 122, 5237–5258. <https://doi.org/10.1002/2016JD026013>.
- Mann, H.B. (1945) Nonparametric tests against trend. *Econometrica*, 13, 245–259. <https://doi.org/10.2307/1907187>.
- McGinley, I. (1982) A diagnosis of Alpine lee cyclogenesis. *Monthly Weather Review*, 110, 1271–1287. [https://doi.org/10.1175/1520-0493\(1982\)110<1271:ADOALC>2.0.CO;2](https://doi.org/10.1175/1520-0493(1982)110<1271:ADOALC>2.0.CO;2).
- McVicar, T.R., Roderick, M.L., Donohue, R.J., Li, L.T., Van Niel, T. G., Thomas, A., Grieser, J., Jhajharia, D., Himri, Y., Mahowald, N. M., Mescherskaya, A.V., Kruger, A.C., Rehman, S. and Dinpashoh, Y. (2012) Global review and synthesis of trends in observed terrestrial near-surface wind speeds: implications for evaporation. *Journal of Hydrology*, 416, 182–205. <https://doi.org/10.1016/j.jhydrol.2011.10.024>.
- McVicar, T.R., Van Niel, T.G., Roderick, M.L., Li, L.T., Mo, X.G., Zimmermann, N.E. and Schmatz, D.R. (2010) Observational evidence from two mountainous regions that near-surface wind speeds

- are declining more rapidly at higher elevations than lower elevations: 1960-2006. *Geophysical Research Letters*, 37, L06402. <https://doi.org/10.1029/2009GL042255>.
- Oke, T.R. (1987) *Boundary Layer Climates*, 2nd edition. New York, NY: Methuen & Co.
- Roderick, M.L., Rotstain, L.D., Farquhar, G.D. and Hobbins, M.T. (2007) On the attribution of changing pan evaporation. *Geophysical Research Letters*, 34, L17403. <https://doi.org/10.1029/2007GL031166>.
- Roulet, Y.-A., Landl, B., Félix, C. and Calpini, B. (2010) Development and challenges in SwissMetNet, the new Swiss meteorological network. In *TECO-2010: WMO Technical Conference on Meteorological and Environmental Instruments and Methods of Observation*. Available at: http://www.wmo.int/pages/prog/www/IMOP/publications/IOM-104_TECO-2010/1_5_%20Roulet_Switzerland.doc [Accessed 15th March 2019].
- Schär, C., Davies, H.C. and Wanner, H. (1998) Present Alpine climate. In: Cebon, P., Dahinden, U., Davies, H.C., Imboden, D.M. and Jäger, C.C. (Eds.) *Views from the Alps: Regional Perspectives on Climate Change*. Boston, MA: MIT Press, pp. 21–72.
- Schwierz, P., Köllner-Heck, E., Mutter, Z., Bresch, D.N., Vidale, P.-L., Wild, M. and Schär, C. (2010) Modelling European winter wind storm losses in current and future climate. *Climate Change*, 101 (3–4), 485–514. <https://doi.org/10.1007/s10584-009-9712-1>.
- Sen, P.K. (1968) Estimates of the regression coefficient based on Kendall's tau. *Journal of the American Statistical Association*, 63, 1379–1389. <https://doi.org/10.2307/2285891>.
- Shaw, T.A., Baldwin, M., Barnes, E.A., Caballero, R., Garfinkel, C.I., Hwang, Y.-T., Li, C., O'Gorman, P.A., Rivière, G., Simpson, I.R. and Voigt, A. (2016) Storm track processes and the opposing influences of climate change. *Nature Geoscience*, 9, 656–664. <https://doi.org/10.1038/ngeo2783>.
- Smith, R.B. (1982) Synoptic observations and theory of orographically disturbed wind and pressure. *Journal of the Atmospheric Sciences*, 39, 60–70. [https://doi.org/10.1175/1520-0469\(1982\)039<0060:SOATOO>2.0.CO;2](https://doi.org/10.1175/1520-0469(1982)039<0060:SOATOO>2.0.CO;2).
- Sprenger, M., Dürr, B. and Richner, H. (2016) Foehn studies in Switzerland. In: *From Weather Observations to Atmospheric and Climate Sciences in Switzerland: Celebrating 100 Years of the Swiss Society for Meteorology*. Zürich: VDF Verlag.
- Stucki, P., Brönnimann, S., Martius, O., Welker, C., Imhof, M., von Wattenwyl, N. and Philipp, N. (2014) A catalog of high-impact windstorms in Switzerland since 1859. *Natural Hazards and Earth System Sciences*, 14, 2867–2882. <https://doi.org/10.5194/nhess-14-2867-2014>.
- Stucki, P., Dierer, S., Welker, C., Gómez-Navarro, J.J., Raible, C.C., Martius, O. and Brönnimann, S. (2016) Evaluation of downscaled wind speeds and parameterised gusts for recent and historical windstorms in Switzerland. *Tellus A*, 68, 31820. <https://doi.org/10.3402/tellusa.v68.31820>.
- Stull, R.B. (1988) *An Introduction to Boundary Layer Meteorology*. Amsterdam: Springer. <https://doi.org/10.1007/978-94-009-3027-8>.
- Theil, H. (1950) A rank-invariant method of linear and polynomial regression analysis. *Koninklijke Nederlandse Akademie van Wetenschappen. Series A. Mathematical Sciences*, 53, 386–392 (part I), 521–525 (part II), 1397–1412 (part III).
- Vautard, R., Cattiaux, J., Yiou, P., Thépaut, J.N. and Ciais, P. (2010) Northern hemisphere atmospheric stilling partly attributed to an increase in surface roughness. *Nature Geoscience*, 3, 756–761. <https://doi.org/10.1038/NNGEO979>.
- Vergeiner, I. and Dreiseitl, E. (1987) Valley winds and slope winds—observations and elementary thoughts. *Meteorology and Atmospheric Physics*, 36, 264–286. <https://doi.org/10.1007/BF01045154>.
- Wan, H., Wang, X.L. and Swail, V.R. (2010) Homogenization and trend analysis of Canadian near-surface wind speeds. *Journal of Climate*, 23, 1209–1225. <https://doi.org/10.1175/2009JCLI3200.1>.
- Wanner, H. and Furger, M. (1990) The bi-se-climatology of a regional wind north of the Alps. *Meteorology and Atmospheric Physics*, 43, 105–115. <https://doi.org/10.1007/BF01028113>.
- Weber, R.O. and Furger, M. (2001) Climatology of near-surface wind patterns over Switzerland. *International Journal of Climatology*, 21, 809–827. <https://doi.org/10.1002/joc.667>.
- Weissmann, M., Braun, F.J., Gantner, L., Mayr, G.J., Rahm, S. and Reitebuch, O. (2005) The Alpine mountain-plain circulation: airborne Doppler Lidar measurements and numerical simulations. *Monthly Weather Review*, 133, 3095–3109. <https://doi.org/10.1175/MWR3012.1>.
- Welker, C. and Martius, O. (2014) Decadal-scale variability in hazardous winds in northern Switzerland since end of the 19th century. *Atmospheric Science Letters*, 15, 86–91. <https://doi.org/10.1002/asl2.467>.
- Whiteman, C.D. (1990) Observations of thermally developed wind systems in mountainous terrain. In: Blumen, W. (Ed.) *Atmospheric Processes Over Complex Terrain. Meteorological Monograph*, 23. Boston, MA: American Meteorological Society, pp. 5–42.
- You, Q., Fraedrich, K., Min, J., Kang, S., Zhu, X., Pepin, N. and Zhang, L. (2014) Observed surface wind speed in the Tibetan Plateau since 1980 and its physical causes. *International Journal of Climatology*, 34, 1873–1882. <https://doi.org/10.1002/joc.3807>.
- Zha, J., Wu, J. and Zhao, D. (2017) Effects of land use and cover change on the near-surface wind speed over China in the last 30 years. *Progress in Physical Geography*, 41, 46–67. <https://doi.org/10.1177/0309133316663097>.
- Zhang, H., Pu, Z. and Zhang, X. (2013) Examination of errors in near-surface temperature and wind from WRF numerical simulations in regions of complex terrain. *Weather Forecast*, 28, 893–914. <https://doi.org/10.1175/waf-d-12-00109.1>.

SUPPORTING INFORMATION

Additional supporting information may be found online in the Supporting Information section at the end of this article.

How to cite this article: Graf M, Scherrer SC, Schwierz C, *et al.* Near-surface mean wind in Switzerland: Climatology, climate model evaluation and future scenarios. *Int J Climatol.* 2019;1–13. <https://doi.org/10.1002/joc.6108>